UNIVERSITI
TEKNOLOGI
MARA

CONFERENCE PROCEEDING

ICITSBE 2012

1ST INTERNATIONAL CONFERENCE ON INNOVATION AND TECHNOLOGY FOR SUSTAINABLE BUILT ENVIRONMENT

16 -17 April 2012

Organized by:
Office of Research and Industrial
Community And Alumni Networking
Universiti Teknologi MARA (Perak) Malaysia
www.perak.uitm.edu.my

PAPER CODE : GT 04

SIMULATION OF DYNAMIC ABSORBED ENERGY ANALYSIS OF MULTI-CELL ALUMINUM 6061-T6 ALLOY EXTRUSION

Akbar Othman[1] and Mohd Fahrul Hasan[2]
[1]Department of Mechanical Engineering, Polytechnic Port Dickson, Malaysia
akbar@polipd.edu.my
[2]Department of Material and Design Engineering, Universiti Tun Hussein Onn Malaysia, Malaysia
fahrul@uthm.edu.my

Abstract
The crushing simulation is presented in this paper to determine the dynamic absorbed energy of multi-cell aluminum 6061-T6 alloy extrusion tubes under axial loading. Thin-walled extruded aluminum 6061-T6 alloy tubes were widely used as energy absorbers for decades since they have an advantage in terms of strength to weight ratio efficiency. The presented paper deals with identifying the influence of the variety of cell on thin-walled tubing as well as variables wall-thickness and velocity impact when subjected to dynamic axial loading. The main focus was on improvement of crush energy absorption of structures in frontal crush impact cars. The numerical simulations of thin-walled tubes were modeled and analyzed using LS-DYNA commercial finite element software. The validation was carried out based on numerical studies from reference literature to ensure that the predictions of modeling analysis were accepted. Results indicated that the thin-walled tube's energy absorption capability was affected significantly by variations in multiple cell, velocity-impact and wall-thickness.

Keywords: Energy Absorption, Thin-Walled Structure, Finite Element Analysis, Multi-cell, Axial Crushing

1.   Introduction

Thin-walled aluminum column are materials of increasing importance because they may have good energy absorption capabilities, as well as other properties such as damping, insulation, specific stiffness and fire retardant properties. This may be important where crashworthiness is a major concern, and knowledge of their dynamic properties would clearly be critical. There is already evidence that using aluminum or steel tubes with variety of shape as well as thin-walled tube hollow section are widely used in application on vehicle such as automotive, ships and aerospace industry. The present work was initiated, therefore, to investigate strain rate effects on the deformation behavior and energy absorption capability of simple thin-walled aluminum 6061-T6 alloy with various cell inside the thin walled tube. It will be shown that strain rate exerts a significant effect upon these parameters. This report also presents several avenues that have been identified for further exploring the high strain rate deformation of thin-walled tubular structure which will be the subjects of future work.

In the present study, numerical analyses were carried out in the present paper to simulate the axial crushing of single-cell, double-cell, triple-cell, and fourth-cell Aluminum 6061-T6 Alloy. The wall-thickness of 1.0, 1.5, and 2.0 mm made of 6061-T6 Aluminum Alloy were selected and examined in term of interaction effect structures. The velocities of dynamic loading were variable at 30 and 45   m/s. Numerical simulations using non-linear explicit finite element code LS-DYNA version 3.71 were carried out and once the numerical results was compared from previous investigation to ensure that the numerical analysis will sufficiently accuracies. Figure 1 shows finite element model of multi cell type A consider one cell centered on tube, type B double cell on three sections, type C divided fourth section, type D centered in center cross-section and type E centered on section on every edge of tubes. The objective in this paper was to determine the comparison crushing absorbed energy with different cell of tubing. The velocity of dynamic impact of 30 and 45 were selected and wall-thickness thin-walled structure of 1.0 and 2.0 mm were examined and investigated. The material of aluminum 6061-T6 alloy was investigated and in the result conclusion the dynamic, mean load and absorbed energy versus displacement curve different were compared and discussed in throughout the papers.
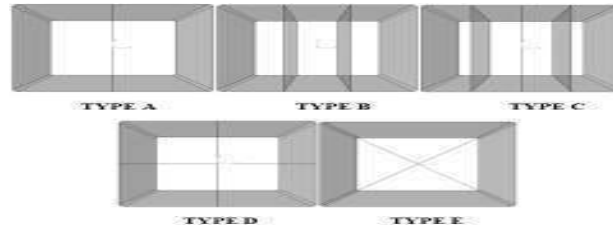
Figure 1: Finite element model for type A, B, C, D and E of multi-cells.

2. Finite element modeling

In this study LS-DYNA version 3.71 was used throughout the analysis. Throughout the simulation process, five differences geometry of tubes have been modeled, which are type of A, B, C, D and E shown in Figure 1. The finite element models and run the crash analyses. In LS-DYNA, the columns' material is modeled as the plastic kinematic hardening model material Type 3 and then the impact contacts among the self-shell elements during these analyses are predicted using the automatic single surface contact algorithm. The single-cell, double-cell triple-cell and fourth-cell columns with sectional width of 35 mm were considered in the analyses see in Figure 1. The wall thickness of the all model column was fixed at 1.0 and 2.0 mm, instead number of cell can give a different weight. The column walls were modeled with shell elements. The interaction between the surface of frontal impact plate and the column shell was simulated with a surface to surface sliding contact. A single surface contact algorithm was used to account for the contact between the lobes of the walls. The axial crushing process was simulated dynamically by a moving rigid wall pushing one end of the column while the other end was simply supported. The column wall material was aluminum extrusion aluminum 6061-T6 alloy. Its mechanical properties and tensile stress–strain data were provided in the Figure 2. The top and bottom plate were modeled using analytical rigid surface to ensure that no effect can be existed during progressive collapse. The value of the velocity and time need to be suitable and the velocity of 30 and 45 m/s were selected and 0.03 was found for calculated for crushing time. Boundary conditions are applied to every regions of the model where there displacements and rotations are known. Such regions may be constrained to remain fixed or may have specified non-zero displacements and rotations. In these models the fixed-free condition has been used where the top section of the tube is constrained completely and, thus, cannot move in any direction also. The bottom section, however, is fixed in the horizontal direction but is free to move in vertical direction.

2.1 Material properties

Numerical analyses were carried out to simulate the axial crushing of aluminum extrusions of aluminum 6061-T6 alloy columns with same weight. Aluminum 6061-T6 alloy was used for column material since the material properties could be modeled as isotropic with good accuracy and negligible strain rate sensitivity was evident for this alloy. The material property was taken from the Figure 2, while the structural geometry is listed in Table 2. All the modeling were 200 mm high (H), 70 x 70 mm of width (D1) and wall thickness were 1.0 mm and 2.0 mm. The analysis of dynamic absorbed energy was calculated using equation (1) and the total work done (W) during the axial crushing of the column are equal to the area under the load-displacement curve and is evaluated as:

$$W = \int Pds \qquad\qquad (1)$$

where, P is the force acting on the tube. Therefore the specific energy absorption per unit mass, E is recognized as:

$$E = \frac{W}{m} \qquad\qquad (2)$$

where, m is the crushed mass of the thin-walled tube.

It was assumed that thin-walled aluminum extrusion has only isotropic strain hardening, and for quasi-static loading, the strain rate effects on the yield strength were neglected due to the relatively low overall average load rate used in the tensile tests. For dynamic loading, the effect of strain rate was included in the finite element model using the Cowper–Symonds constitutive equation given by the following relation:

$$\dot{\varepsilon}_p = D^t \left(\frac{\sigma_d}{\sigma_s} - 1 \right)^{q^t} \; for \mapsto \sigma_d \geq \sigma_s \tag{3}$$

where σ_d is the dynamic flow stress at a uniaxial plastic strain rate ε_p, σ_s, the associated static flow stress, and the constants D^t and q^t are tube material parameters. Equation (3) is an overstress power law that was incorporated into the finite element model.

Table 1: Material properties of mild steel (validation)

General dimension multi-cell	
Length (mm)	200
Width (mm)	70 x 70
Velocity (m/s)	30 and 45
Wall-Thickness (mm)	1.0, 2.0

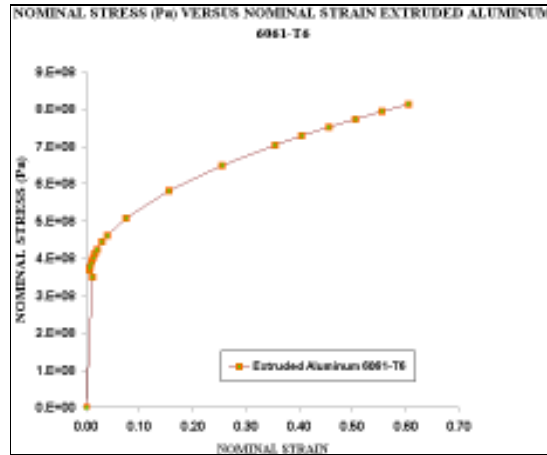| Steel	Stress (Pa)	Strain
E (Pa) (207E9)	1.587E8	0.0
	1.631E8	0.015
Density (kg/m3)	1.863E8	0.033
7800	1.932E8	0.044
Poisson ratio (0.3)	2.020E8	0.062
	2.070E8	1.500

Figure 2: Nominal stress and strain curve of extruded aluminum 6061-T6 alloy

2.2   Crushing process and Validation of finite element model

The simulation, which normally is run as a background process, is a stage in which LS-DYNA the numerical problem defined in the model. LS-DYNA is a special-purpose analysis product that uses an explicit dynamic finite element formulation. It is suitable for short, transient dynamic events, such as impact and blast problems, and is also very efficient for highly nonlinear problems involving changing contact conditions, such as forming simulation. It is well known that a nonlinear structural problem is one in which the structure's stiffness changes as it deforms. All physical structures are nonlinear. In this simulation the stiffness is fully dependent on the displacement; the initial flexibility can no longer be multiplied by the applied load to calculate the spring's displacement for any load. Results evaluation can be done once the simulation has been completed and the reaction forces, displacements, energy or other fundamental variables have been calculated. The evaluation is generally done interactively using the visualization module of LS-POST. The visualization module, which reads the neutral binary output database file, has a variety of options for displaying the results, including color contour plots, animations, deformed shaped plots, and X–Y plots.
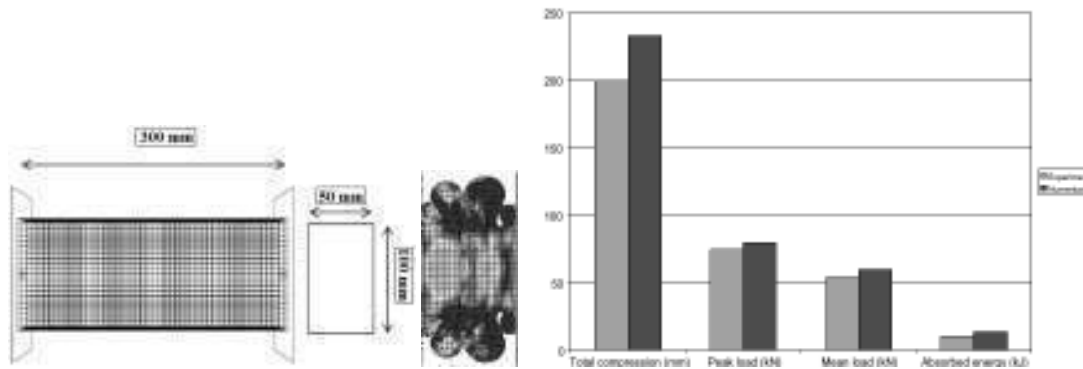
Figure 3: Finite element model of validation

The validation of finite element model was carried out using existing experimental by Abramowicz and Jones. A model of steel straight rectangular tube was developed using finite element model of LS-DYNA code with the free length of the tube being 300 mm, while the cross-section dimensions were 100 x 50 mm illustrated in Figure 3. The tube thickness is 1.5 mm and loaded with impact mass of 90 kg at a velocity of 15 m/s. Figure 3 also shows a complete crushing of a rectangular tube and the failure mechanism of the tube. As the number of lobes produced were 2.5 in symmetrical manner. The validation is of particular importance, since it proves that the simulation model can be effectively used to examine the failure mechanism of a crushed tube. The tube response obtained by the finite element model was compared with that of the theoretical model for a range of crash parameters under dynamic loading as shown in Figure 3. The crash parameters that have been analyzed were total compression, peak load, mean load, and total energy absorbed by the tube. Numerical results show a higher value as compared to experimental one. It can also be seen that the difference between value of experiment and numerical analysis from the table above can be considered as reasonable as listed in Figure 3.

3.   Results and Discussion

The axial crushing of hollow multi-cell columns was addressed in the present paper. Based on an analytical solution for the mean crushing and dynamic loading of multi-cell sections were derived, and the result was compared very well with the different cell of tubing. It was found that the influence number of cell in interaction effects between the frontal crash plate and the column wall contribute to the total crushing resistance by the amounts equal to 80% and 90% of the direct resistance for type A, B, C, D and E of multi-cell respectively. The energy absorption during the axial crushing up to the effective stroke length can be calculated using the expressions of the mean crushing force where (EA) is the energy absorption, (Pm) is the mean crushing load, (L) denotes the length of the column, (SE) is the stroke efficiency as mentioned previously. Failure mechanisms of multi-cell of tubing were observed through five different numbers of cell produce onto tube hollow which were type A, type B, type C, type D and type E. Interpreting the collapse manner of every tubes, there was difference in their behavior due to the tubes geometry. Apart from the multi-cell tube, failure mechanism for tube shows different characteristics.

Although there were five different tubes being tested for the failure mechanism for all the tubes and can be classified into one identical mode. Figure 5 represents the failure mechanism of the multi-cell tube. At the initial crush step (0 mm), the bottom end of the tube bent outward as the tube geometry was modeled to initiate the first step of crushing. Therefore, the lower section with a straight part is now in contact with the plate. As the collapse progresses, the third, post crush (50 mm), and fourth step, middle post crush (120 mm) of failure takes place and as the tube's structure needs to overcome the friction between the straight part and the plate, the structure fails at the middle section.

TYPE A   **TYPE B**

590

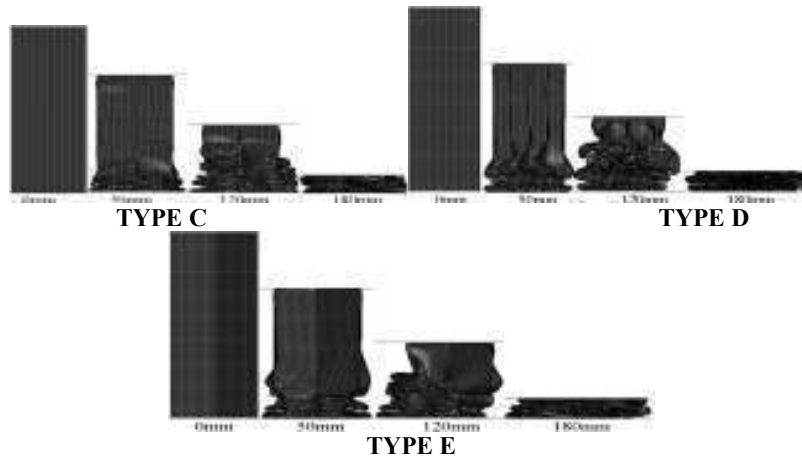**TYPE C**   **TYPE D**

TYPE E
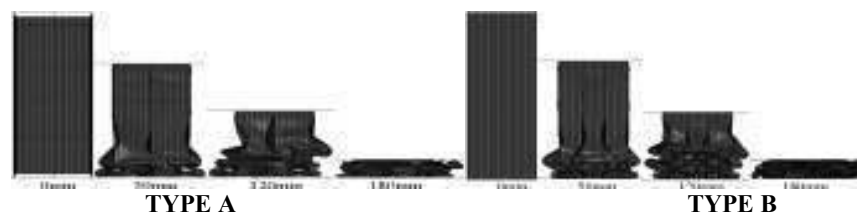
Figure 4: Deformation pattern type of A, B, C, D and E (Wall-thickness = 1.0 mm: velocity 30 m/s)

In the middle post crush step, it can be seen that the straight part of the tube's wall moves horizontally inwards and gets in contact with each other, hence forcing the lobe part to fold vertically. This process will reoccur at the upper section of the tube but in different orientation than the one that occurred below it. In the post crush step, the amount of energy absorbed by the multi-cell tube will be controlled by the crush failure propagation mechanism. As the tube continues to fold, the structure undergoes material densification stage, which reduces its capability to absorb energy. This can be observed in the fifth step of the crushing process (180 mm). In the final crush step the structure can no longer absorb more energy since it becomes undeformable or completely behaves as a rigid body. Load displacement curves of crushing characteristics of the tubes can be explained by their load displacement curves.
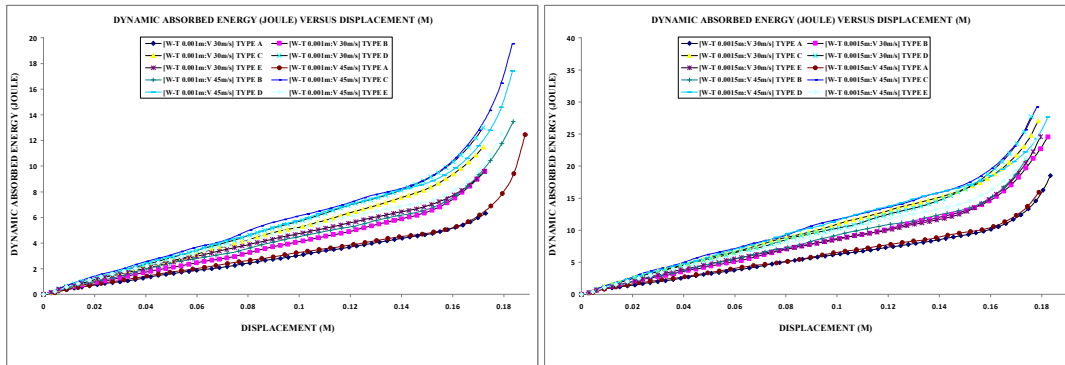

(Wall-Thickness 1.0 mm)

(Wall-Thickness 1.5 mm)
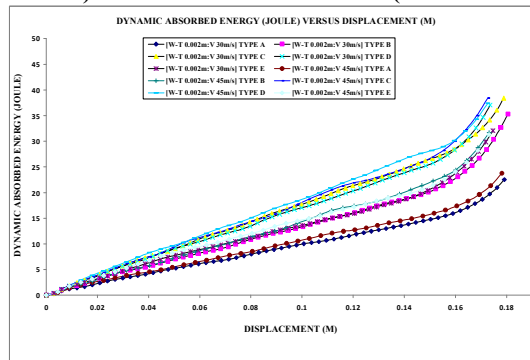
591
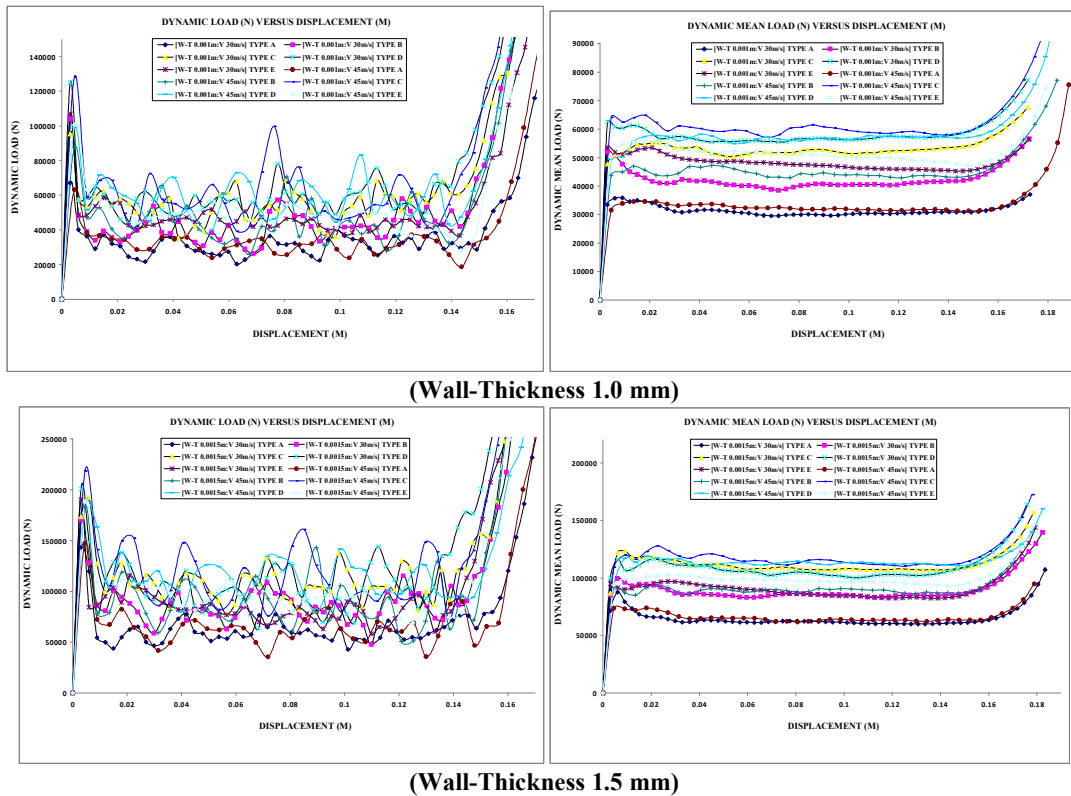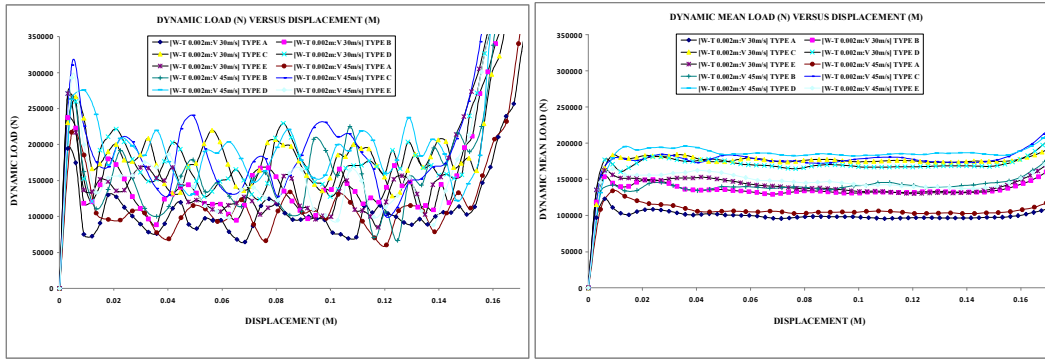
(Wall-Thickness 2.0 mm)

Figure 5: Dynamic and mean load (N) versus displacement (m) type A, B, C, D and E (Wall-thickness = 1.0, 1.5 and 2.0 mm: velocity 30 and 45 m/s)

The initial buckling load of the tubes corresponds to the peak load in the first buckling-cycle. In practice, this load is very important for crashworthiness design that gives an indication of the force required to initiate collapse and hence begin the energy absorption process. The curve for metallic multi-cell tube is shown in Figure 5. These figures show highly non-uniform character where the height of the first buckling cycle is significantly bigger than the subsequent buckling cycle. This high fluctuations and the overshoot in the load displacement curve was contributed by the elastic stiffness of the metallic tube. It can be observed that the initial elastic deformation phase, during which the load rises steeply at a steady rate up to a peak value, Pmax. As for the metallic multi-cell tubes, the post crushing region of the load displacement curves is characterized by a stable and uniform manner. These curves can be divided into four stages. First stages represent the pre-crush stage and the second one shows failure initiation crush-stage where the collapse is first observed at the bottom part of the tubes. The initial failure crush occurs as the load displacement curves experience a significant change in their slope. Crush failure propagation mechanism is established in the third stage which is post-crush failure stage and it controls the accumulation energy absorbed by multi-cell tubes. The mean crushing forces up to the effective stroke length were calculated for the columns. As can be seen in Figure 5 left side, the effective stroke length at which the crushing force rises steeply varies slightly for different cell produce onto hollow tube.

(Wall-Thickness 1.0 mm)

(Wall-Thickness 1.5 mm)

(Wall-Thickness 2.0 mm)

592

Figure 6: Dynamic absorbed energy (Joule) versus displacement (m) type A, B, C, D and E (Wall-thickness = 1.0, 1.5 and 2.0 mm: velocity 30 and 45 m/s)

3.1 Dynamic absorbed energy calculation

The analysis of dynamic absorbed energy was calculated using equation (1) and the total work done (W) during the axial crushing of the column are equal to the area under the load-displacement. Figure 6, an ideal energy absorbing design should provide a desirable constant mean crush mean load distance response under an axial loading. Generally, the initial peak in the crush force and crush distance response represents the maximum crush force (Pmax) that typically occurs soon after the start of the crush process and is due to the initial elastic resistance. While it is desirable to increase energy absorption, it is preferable to decrease Pmax in search of an optimum tube design. Moreover if tube remains fairly straight during the crush process, its energy absorption capacity will be slightly maintain during progressive collapse. The resulting energy absorption is plotted in Figure 6. A few observations can be made based upon the energy absorption plot. The multi-cell section type of D sections generally exhibit higher energy absorption values and thus higher weight efficiency in energy absorption. The gain in energy absorption type of D cell and the C and E cell is about 30 – 70 % compared to the type of A and B cell. The type of D cell is better than the type of E cell in terms of energy absorption. It should be noted that the comparison in Figure 6 are based on one fixed sectional cross-section and a same wall-thickness as well as velocity of impact.

4. Conclusions

In this study, the finite element modeling of the axial crushing of aluminum 6061-T6 alloy, multi-cell type of A, B, C, D and E tubes section were developed and examined very well using the LS-DYNA explicit version 3.71 code. The dynamic crushing, dynamic mean load and energy absorption performance were presented and discussed in detail. The following concluding remarks may be drawn:

1) Multi-cell type of D exhibit the highest amount of energy absorbed from the crushing rather than C, E, B and A.
2) Tube with multi-cell type of D collapse in a stable, progressive and controlled manner, therefore, it can dissipate a large amount of energy.
3) Crashworthiness behavior of the multi-cell tube is being influenced by the tube wall-thickness as the value of dynamic velocity of impact, total energy absorbed by the tube increase.

Acknowledgment

References

Wierzbicki T, Abramowicz W. On the crushing mechanics of thin-walled structures. Journal of Applied Mechanics 1983;50:727–39.

Abramowicz W, Wierzbicki T. Axial crushing of multicorner sheet metal columns. Journal of Applied Mechanics 1989;56:113–20.

Chen W, Nardini D. Experimental study of crush behavior of sheet aluminum foam-filled sections. International Journal of Crashworthiness 2000;5(4).

Seitzberger M, Rammerstorfer FG, Degischer HP, Gradinger R. Crushing of axially compressed steel tubes filled with aluminum foams. Acta Mechanica 1997;125:93–105.

Seitzberger M, Rammerstorfer FG, Gradinger R, Degischer HP, Blaimschein M, Walch C. Experimental studies on the quasi-static axial crushing of steel columns filled with aluminum foam. International Journal of Solids and Structures 2000;37:4125–47.

Hanssen AG, Langseth M, Hopperstad OS. Static crushing of square aluminum extrusions with aluminum foam filler. International Journal of Mechanical Sciences 1999;41(9):967–97.

Hanssen AG, Langseth M, Hopperstad OS. Static and dynamic crushing of circular aluminum extrusions with aluminum foam filler. International Journal of Impact Engineering 2000;24:475–507.

Santosa S, Wierzbicki T. Crash behavior of box column filled wih aluminum honeycomb or foam. Computers and Structures 1998;68(4):343–68.

Santosa S, Wierzbicki T, Hanssen AG, Langseth M. Experimental and numerical studies of foamfilled sections. International Journal of Impact Engineering 2000;24:509–34.

Wierzbicki T. Lecture notes on structural mechanics. Massachusetts Institute of Technology, 1998.

LS-DYNA Keyword User's Manual, version 9.71, Livermore Software Technology Corporation, 2007